Common Reflection Surface Analysis

Paraxial approximation for the time of flight of signals traveling in a 2D acoustic medium

Ernesto Bonomi
EIS-CRS4

Introduction

I present the derivation in the *midpoint-offset* domain of two formulae approximating, for a shot-receiver pair, the *time of flight* of acoustic signals traveling in a 2D non-homogeneous medium. The first expression assumes a *flat* acquisition surface, while the second, which generalizes the first one, takes into account the *topography* of the ground.

Both formulations are based on the approximated kinematic primary response of a reflector segment located around the incidence point of a *reference normal ray*. The approximation requires the use of three parameters: α, R_{NIP} and R_N.

The problem is first solved in an *auxiliary* homogeneous medium; the resulting time of flight is then delayed to be accommodated to the final velocity macro-model.

The resulting expression of the traveltime surface $t(x_m, h)$ is known in the litterature as *Common Reflection Surface.*

Part 1: Case of a flat acquisition surface

These notes were largely inspired by the article presented by G. Höcht, E. de Bazelaire, P. Majer and P. Hubral (1999). I completely derived their work following their steps but trying to be more pedagogic, especially in the section dedicated to the use of an earth auxiliary model for the time of flight correction of seismic signals in real media.

Primary reflections in a 2D non-homogeneous medium

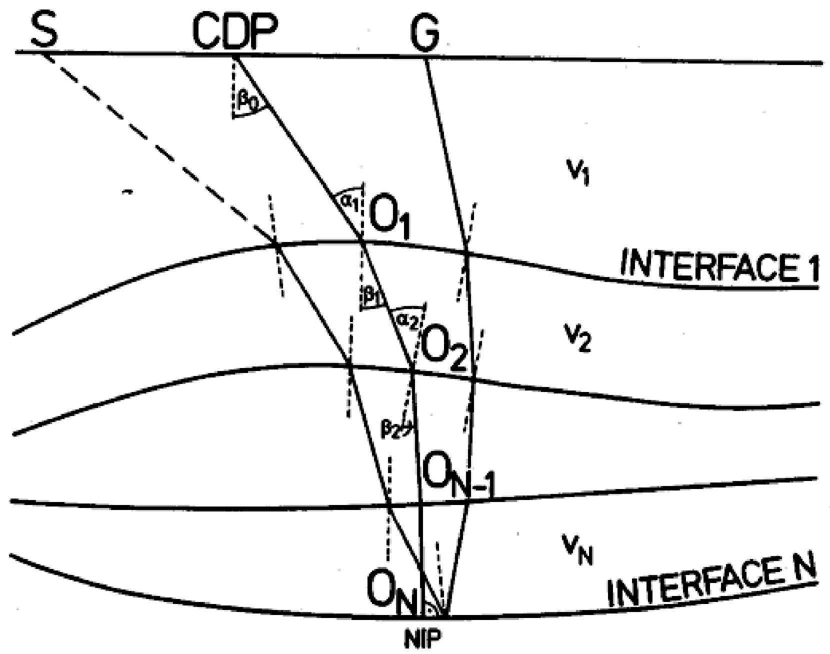

Figure 1: Snell's law governing rays crossing boundaries in a isotropic medium

$$\frac{\sin \alpha_i}{v_i} = \frac{\sin \beta_i}{v_{i+1}}$$

Time of flight for a pair (S, G): analysis in a constant-velocity medium

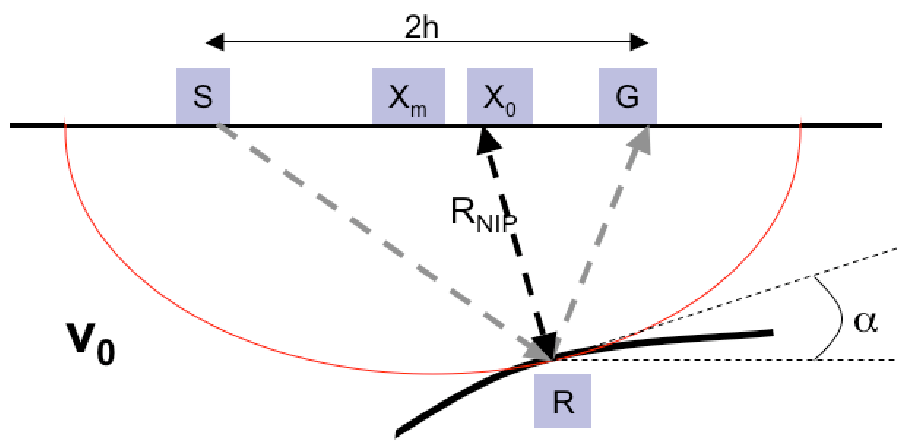

Figure 2: Kinematic response of the reflector: NIP-ray at point R with deep α

Problem: determine the line of equal reflection time, $\overline{SR} + \overline{RG} = v_0 t = 2a$, an *ellipse* tangent to the reflector at point R:

$$\frac{(x_R - x_m)^2}{a^2} + \frac{y_R^2}{a^2 - h^2} = 1, \quad y_R \tan\alpha = -(x_R - x_m)\left(1 - \frac{h^2}{a^2}\right) \tag{1}$$

$$x_R = x_0 + R_{NIP}\ \sin\alpha, \quad y_R = -R_{NIP}\ \cos\alpha, \quad R_{NIP} = \overline{X_0 R},$$

where $2h$ is the acquisition offset, x_m the midpoint and α the reflector deep at R.

Solving system (1) in a^2 and x_m, one finds the following two fundamental relations:

$$t^2(\alpha, h) = \left(\frac{4h}{v_0}\right)^2 + 2\left[\frac{R_{NIP}(\alpha)}{v_0}\right]^2 \left\{\sqrt{\left[\frac{h}{\Gamma(\alpha)}\right]^2 + 1} + 1\right\}, \tag{2}$$

$$x_m(\alpha, h) = x_0(\alpha) + \Gamma(\alpha) \left\{\sqrt{\left[\frac{h}{\Gamma(\alpha)}\right]^2 + 1} - 1\right\}, \tag{3}$$

where

$$\Gamma(\alpha) = \frac{R_{NIP}(\alpha)}{2 \sin \alpha}. \tag{4}$$

Remark: moving point R along the reflector, see figure (3), changes α near the reference deep α_0, providing a family of NIP-rays around the reference one defined by $R_{NIP} = R_{NIP}(\alpha_0)$ and $x_0 = x_0(\alpha_0)$.

Objective: compute t as a function of x_m and h around the *reference* NIP-ray, by eliminating α between (2) and (3).

Approximating x_0 and R_{NIP} along a constant-curvature neighborhood of R

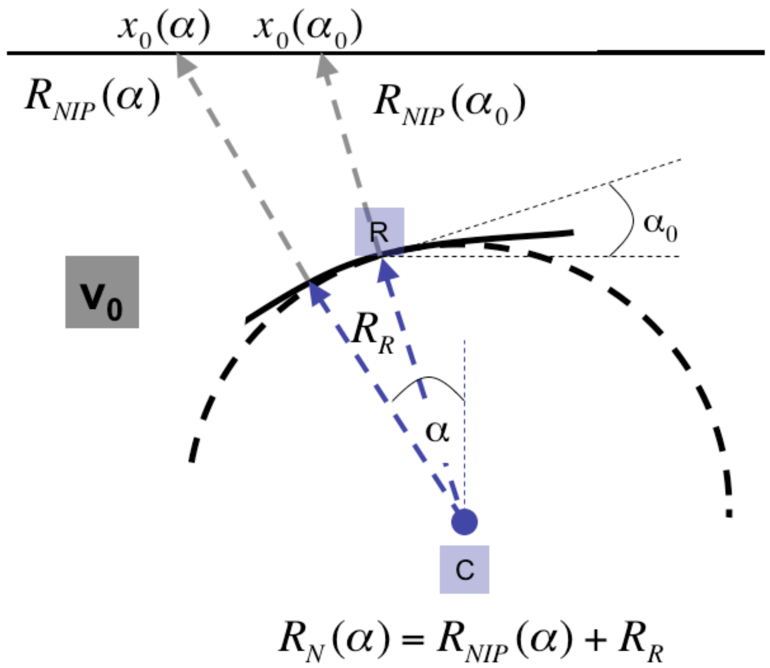

Figure 3: Constant velocity model: small variations around a reference deep α_0

$$R_{NIP}(\alpha) = R_{NIP} + R_N \left(\frac{\cos \alpha_0}{\cos \alpha} - 1 \right), \tag{5}$$

$$x_0(\alpha) = x_0 - R_N \left(\cos \alpha \tan \alpha_0 - \sin \alpha \right). \tag{6}$$

Paraxial approximation of the kinematic response

The paraxial approximation: development of the time of flight $t(\alpha, h)$ and the midpoint $x_m(\alpha, h)$ in power series near the reference NIP-ray at point R.

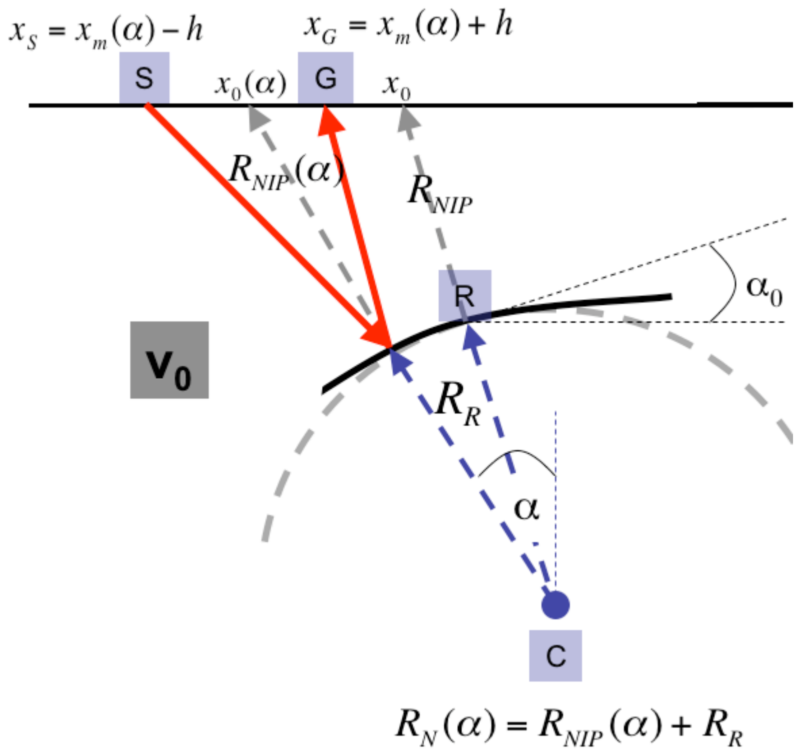

Figure 4: Kinematic response of the reflector near the reference NIP-ray at point R

Remark 1: around the reference NIP-ray, $R_{NIP}(\alpha)$ and $x_0(\alpha)$ are constrained to satisfy the two auxiliary equations (5) and (6).

Remark 2: seismic reciprocity principle, $t(\alpha, h) = t(\alpha, -h)$, imposes that the *Taylor-series expansion* of t must contain only even powers of h:

$$\begin{aligned} t(\alpha, h) &= \frac{2R_{NIP}}{v_0} + \frac{\partial t(\alpha_0, 0)}{\partial \alpha}(\alpha - \alpha_0) + \\ & \quad \frac{\partial^2 t(\alpha_0, 0)}{\partial \alpha^2}(\alpha - \alpha_0)^2 + \frac{\partial^2 t(\alpha_0, 0)}{\partial h^2} h^2 + O(3). \end{aligned} \tag{7}$$

The same is true for the midpoint Taylor-series expansion, since $x_m(\alpha, h) = x_m(\alpha, -h)$.

Remark 3: the *inversion* of the midpoint approximation will be used to map

$$(\alpha - \alpha_0, h) \mapsto (x_m - x_0, h),$$

and, finally, represent (7) as a function of the two acquisition parameters (x_m, h).

Paraxial approximation, first case: $h = 0$

Observe that under this hypothesis equations (2) and (3) take the simple form

$$t(\alpha) = \frac{2R_{NIP}(\alpha)}{v_0} \quad \text{and} \quad x_m(\alpha) = x_0(\alpha),$$

from where, via equations (5) and (6), we can compute the two second-order Taylor-series expansions

$$\begin{aligned} t(\alpha) &= \frac{2R_{NIP}}{v_0} + \frac{2R_N}{v_0} \tan\alpha_0(\alpha - \alpha_0) + \\ &\quad \frac{R_N}{v_0}\left(1 + 2\tan^2\alpha_0\right)(\alpha - \alpha_0)^2 + O(3), \end{aligned} \tag{8}$$

$$x_m(\alpha) = x_0 + \frac{R_N}{\cos\alpha_0}(\alpha - \alpha_0) + \frac{R_N \sin\alpha_0}{\cos^2\alpha_0}(\alpha - \alpha_0)^2 + O(3), \tag{9}$$

which provide time of flight and midpoint estimates for ray trajectories near the reference NIP-ray.

Inversion theorem and Lagrange formula

Hypothesis: let $x_m(\alpha)$ be analytic at $\alpha = \alpha_0$, $x_m(\alpha_0) = x_0$, and $x'_m(\alpha_0) \neq 0$.

Conclusion: then the equation $x = x_m(\alpha)$ has a *unique* solution $\alpha = X_m(x)$ such that $X_m(x_0) = \alpha_0$. This is a standard theorem in complex analysis.

Since x_m and X_m are analytic at $\alpha = \alpha_0$ and $x = x_0$, they can be expanded in power series,

$$x_m(\alpha) = p_0 + p_1(\alpha - \alpha_0) + p_2(\alpha - \alpha_0)^2 + \cdots,$$

$$X_m(x) = P_0 + P_1(x - x_0) + P_2(x - x_0)^2 + \cdots,$$

that converge in the neighborhood of α_0 and x_0. Clearly $p_0 = x_0$ and $P_0 = \alpha_0$, and the highest coefficients P_k can be found by equating coefficients in the identity

$$\alpha - \alpha_0 = \sum_{i=k}^{\infty} P_k \left[\sum_{j=1}^{\infty} p_j (\alpha - \alpha_0)^j \right]^k .$$

A general formula for P_k was found by *Lagrange* in 1768:

$$P_k = \frac{1}{k!} \left\{ \frac{d^{k-1}}{d\alpha^{k-1}} \left[\frac{\alpha - \alpha_0}{x_m(\alpha) - x_0} \right]^k \right\}_{\alpha=\alpha_0}, \text{ for } k = 1, 2, \cdots. \tag{10}$$

Paraxial approximation, first case: $h = 0$ (second part)

Using Lagrange formula (10), the *inversion* of (9) provides the following relation between α and x_m, valid in the neighborhood of the reference NIP-ray:

$$\alpha - \alpha_0 = \frac{\cos\alpha_0}{R_N}(x_m - x_0) - \frac{\sin\alpha_0\cos\alpha_0}{R_N^2}(x_m - x_0)^2 + O(3). \tag{11}$$

By substituting (11) into equation (8), the *zero-offset* time of flight for *homogeneous* media can now be represented as a function of the midpoint coordinate x_m:

$$t(x_m) = 2\,\frac{R_{NIP}}{v_0} + 2\,\frac{\sin\alpha_0}{v_0}(x_m - x_0) + \frac{\cos^2\alpha_0}{v_0 R_N}(x_m - x_0)^2 + O(3), \tag{12}$$

$$\begin{aligned} t^2(x_m) &= 4\,\frac{R_{NIP}^2}{v_0^2} + 8\,\frac{R_{NIP}\sin\alpha_0}{v_0^2}(x_m - x_0) + \\ &\quad 4\,\frac{R_{NIP}\cos^2\alpha_0 + R_N\sin^2\alpha_0}{v_0^2 R_N}(x_m - x_0)^2 + O(3). \end{aligned} \tag{13}$$

Equations (12) and (13) are respectively called the *parabolic* and the *hyperbolic* zero-offset expansions.

Paraxial approximation, second case: $x_m = x_0$

Under this hypothesis, equation (3) takes the form

$$x_0 - x_0(\alpha) = \Gamma(\alpha)\left\{\sqrt{\left[\frac{h}{\Gamma(\alpha)}\right]^2 + 1} - 1\right\} = R_N\left(\cos\alpha\tan\alpha_0 - \sin\alpha\right), \qquad (14)$$

where $x_0(\alpha)$, near the reference NIP-ray, is given by (6).

Observe that after a simple algebraic manipulation of equation (14), we can isolate h^2, which, for small angular variations around α_0, can be written as

$$h^2 = -\frac{R_{NIP}R_N}{\sin\alpha_0\cos\alpha_0}(\alpha - \alpha_0) + O(2),$$

so that, for $x_m = x_0$, we obtain after inversion

$$\alpha - \alpha_0 = -\frac{\sin\alpha_0\cos\alpha_0}{R_{NIP}R_N}h^2 + O(4). \qquad (15)$$

Paraxial approximation, second case: $x_m = x_0$ (second part)

Eliminating the square-root between equations (2) and (14), and expanding $t^2(\alpha, h)$ in Taylor-series around α_0, we obtain:

$$t^2(\alpha, h) = 4\frac{R_{NIP}^2 + h^2}{v_0^2} + 4\tan\alpha_0 \frac{R_{NIP}R_N}{v_0^2}(\alpha - \alpha_0) + O(2). \qquad (16)$$

After the substitution of (15) into (16), the approximated *hyperbolic* time of flight in for *homogeneous* media can be represented as a function of the acquisition offset h:

$$t^2(h) = \left(\frac{2R_{NIP}}{v_0}\right)^2 + 4\,\frac{\cos^2\alpha_0}{v_0^2}\,h^2 + O(4). \qquad (17)$$

From this last expression, approximating the square-root of (17) to the second order in h, we obtain the *parabolic* expansion of the time of flight:

$$t(h) = 2\,\frac{R_{NIP}}{v_0} + \frac{\cos^2\alpha_0}{v_0\,R_{NIP}}\,h^2 + O(4). \qquad (18)$$

Time of flight in homogeneous media: paraxial approximation

From the Taylor-series expansion (7), collecting (12) and (18), we obtain the *parabolic* approximation, valid near the reference NIP-ray in constant-velocity media:

$$t(x_m,h) = \frac{2R_{NIP}}{v_0} + \frac{2\sin\alpha_0}{v_0}(x_m - x_0) + \frac{\cos^2\alpha_0}{v_0 R_N}(x_m - x_0)^2 + \frac{\cos^2\alpha_0}{v_0\ R_{NIP}}\ h^2 + O(3). \quad (19)$$

Similarly, using (13) and (17), we derive the *hyperbolic* approximation of the time of flight:

$$\begin{aligned} t^2(x_m,h) \quad = \quad & \left(\frac{2R_{NIP}}{v_0}\right)^2 + \frac{8R_{NIP}\sin\alpha_0}{v_0^2}(x_m - x_0) + \\ & 4\ \frac{R_{NIP}\cos^2\alpha_0 + R_N\sin^2\alpha_0}{v_0^2 R_N}(x_m - x_0)^2 + \\ & \frac{4\cos^2\alpha_0}{v_0^2}\ h^2 + O(3). \end{aligned} \quad (20)$$

The objective now is to adapt equations (19) and (20) to the more general case of a laterally inhomogeneous medium.

Non-homogeneous medium

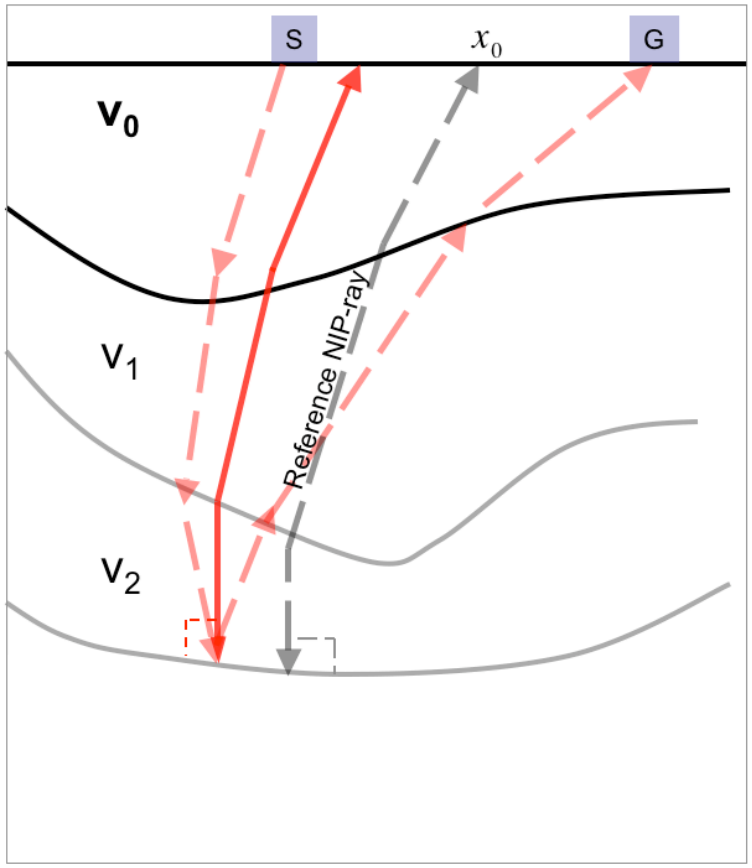

Figure 5: Kinematic of a laterally inhomogeneous medium.

Homeomorphic models

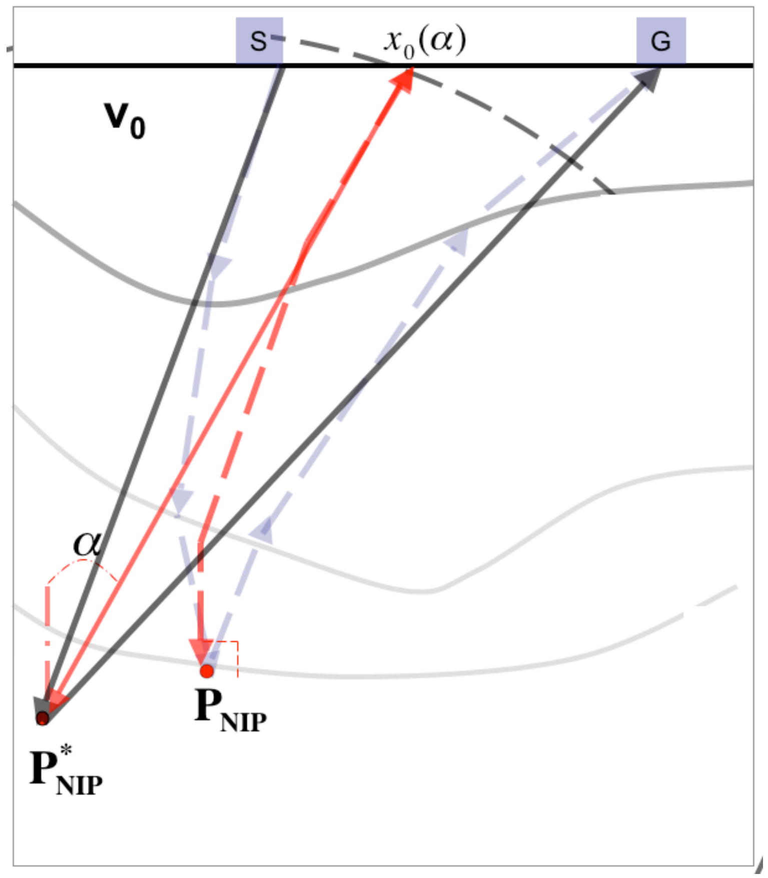

Figure 6: Kinematic of quasi similar subsurface models: the image point P^*_{NIP} of P_{NIP} is determined by the *direction* and the *radius of curvature* of the t*rue* NIP-wavefront.

Kinematics of quasi similar subsurface models

Let us find a relation between the time of flight $t(x_m, h)$ of a signal traveling in a non-homogeneous medium *with* a constant near-surface velocity v_0, see figure (5), and the traveltime $t_A(x_m, h)$, provided by equation (19) and (20), of a signal propagating in an *auxiliary* homogeneous medium where $v = v_0$, see figure(6).

Both wavefronts *initiated* at P_{NIP} and P^*_{NIP} are *locally identical* when they emerge at the surface but they are *delayed* because of the different action of the two media.

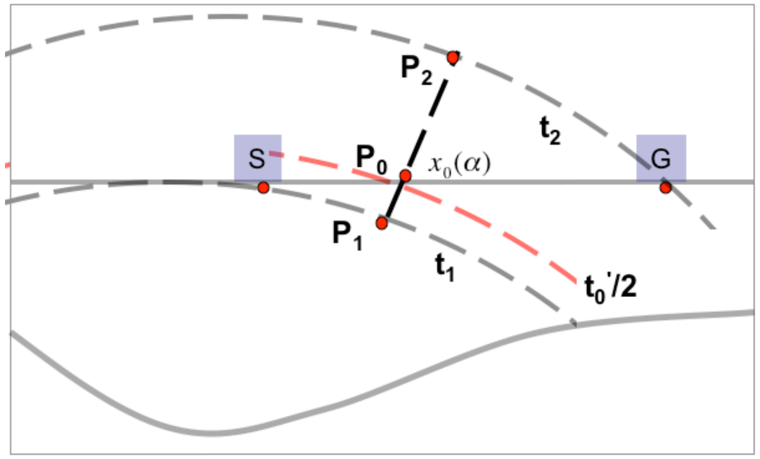

Figure 7: NIP-wavefronts at three different instants of time: emerging at the source position, at $x_0(\alpha)$ and at the receiver position, see figure(6).

Time delay between real and auxiliary media (I)

The kinematic illustrated in figure (7) is the same for both media, the *real* and the *auxiliary* one. In particular, making the two following assumptions,

(i) the emerging NIP-wave in *locally circular* and

(ii) it propagates with a *constant velocity* v_0 near the ground surface,

we have that:

$$\overline{P_0P_1} = \left(\frac{t_0'}{2} - t_1\right) v_0, \quad \overline{P_2P_0} = \left(t_2 - \frac{t_0'}{2}\right) v_0,$$

where for both media $t_1 + t_2$ is the source-receiver time of flight while t_0' is the NIP-ray traveltime.

Hence the quantity $\overline{P_2P_0} - \overline{P_0P_1} = (t_1 + t_2 - t_0')v_0$ is *preserved* in both media, so that we may write:

$$\begin{aligned} \frac{\overline{P_2P_0} - \overline{P_0P_1}}{v_0} &= t(x_m, h) - t_0(\alpha) \\ &= t_A(x_m, h) - \frac{2R_{NIP}(\alpha)}{v_0}. \end{aligned} \tag{21}$$

Time delay between real and auxiliary media (II)

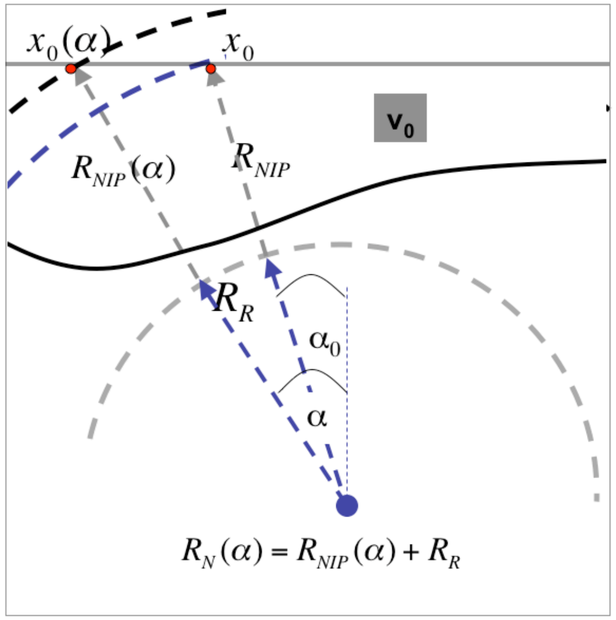

Figure 8: NIP-waves locally circular and concentric for both *real* and *auxiliary* media.

Assuming that both NIP-waves, when emerging at x_0 and at $x_0(\alpha)$, are *locally circular* and *concentric*, see figure (8), the time difference between these two events can be computed monitoring the propagation of an N-wave in the *auxiliary* subsurface model.

Time delay between real and auxiliary media (III)

As illustrated in figure (8), we find the following time difference, valid for small angular deviations around α_0:

$$
\begin{aligned}
t_0(\alpha) - t_0 &= \frac{2}{v_0}\left[R_N(\alpha) - R_N\right] \\
&= \frac{2}{v_0}\left[R_{NIP}(\alpha) - R_{NIP}\right]
\end{aligned} \tag{22}
$$

Finally, combining equations (21) and (22), we obtain the fundamental *time correction* to t_A,

$$
t_A(x_m, h) = t(x_m, h) - \left(t_0 - \frac{2R_{NIP}}{v_0}\right). \tag{23}
$$

This last relation allows the estimate of the time of flight for a signal traveling in a real medium.

Paraxial approximation of the time of flight in non-homogeneous media

With the help of the auxiliary model, using the time correction (23), equations (19) and (20) provide an estimate of the time of flight in *non-homogeneous* media where the sound velocity v_0 near the ground surface is constant.

Consequently, the *parabolic* approximation takes the form

$$t(x_m, h) = t_0 + \frac{2\sin\alpha_0}{v_0}(x_m - x_0) + \frac{\cos^2\alpha_0}{v_0 R_N}(x_m - x_0)^2 + \frac{\cos^2\alpha_0}{v_0\ R_{NIP}}\ h^2 + O(3), \quad (24)$$

while the *hyperbolic* one becomes

$$\begin{aligned} \left[t(x_m,h) - \left(t_0 - \frac{2R_{NIP}}{v_0}\right)\right]^2 \quad = \quad & \left(\frac{2R_{NIP}}{v_0}\right)^2 + \frac{8R_{NIP}\sin\alpha_0}{v_0^2}(x_m - x_0) + \\ & 4\ \frac{R_{NIP}\cos^2\alpha_0 + R_N\sin^2\alpha_0}{v_0^2 R_N}(x_m - x_0)^2 + \\ & \frac{4\cos^2\alpha_0}{v_0^2}\ h^2 + O(3). \end{aligned} \quad (25)$$

Both expansions depend, for each point (x_0, t_0) of the *zero-offset* section, on three parameters, (α, R_{NIP}, R_N), whose values are those for which the traveltime surface fits best the reflection events. The use of (25) is highly recommended for its accuracy.

Part 2: Case of an acquisition surface with topography

The results presented in these notes were inspired by the article presented by P. Chira, M. Tygel, Y. Zhang and P. Hubral. I derived their work in a completely different way, following step by step the approach presented in the first part of this document, then using the concept of auxiliary model.

Acquisition with topography in a homogeneous medium

I present the paraxial approximation for the time of flight of signals traveling in a 2D media with topography and derive formulas for the homogeneous case.

The case of a non-homogeneous medium can be solved by delaying, exactly as we did before, the time of flight corresponding to the auxiliary subsurface model.

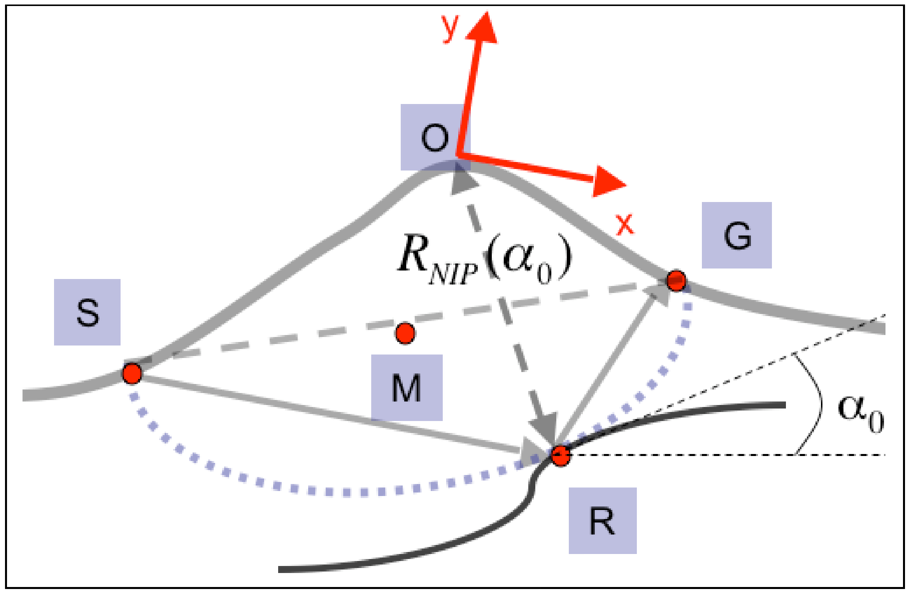

Figure 9: Acquisition with topography, kinematic response of point R with deep α_0: NIP-ray emerging at point O.

Curved measurement surface

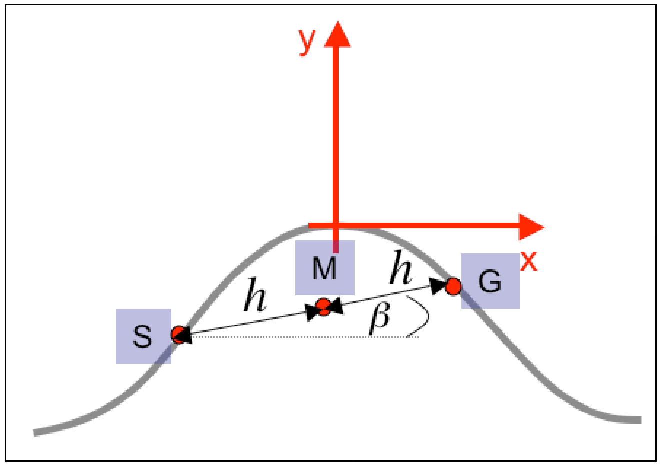

Figure 10: The local reference system is tangent to the surface.

We adopt a *local* coordinate system, tangent to the surface and centered at x_0 (the emerging point of the reference NIP-ray), figures (9). At the origin of the axis, the surface has a *curvature* $\kappa = 2K$, so that, the topography, see figure (10), may be *locally* approximated by the *parabola*

$$y(x) = -Kx^2. \tag{26}$$

The local reference system

Under the assumption of regularity of the topography, equation (26), in the local reference system the two midpoint coordinates take the form:

$$x_m = -\frac{\tan\beta}{2K}, \quad y_m = -K\left(x_m^2 + h^2\cos^2\beta\right). \tag{27}$$

Eliminating β between equations (27), we see that the time of flight t is a function of only two variables, x_m and the acquisition offset h.

The reciprocity principle imposes that the Taylor-series expansion of t must contain only *even* powers of h.

This means that, to construct the second-order expansion of t, by analogy with equation (7), we can *again* discriminate the two acquisition configurations

- $h = 0$ with the midpoint coordinate $y_m = -Kx_m^2$,
- $x_m = 0$ with the midpoint coordinate $y_m = -Kh^2$.

Remark: in the local reference system, the second case is equivalent to set $\alpha = \alpha_0$.

Computing $x_0(\alpha)$ and $R_{NIP}(\alpha)$ for a NIP-ray reaching the curved surface (I)

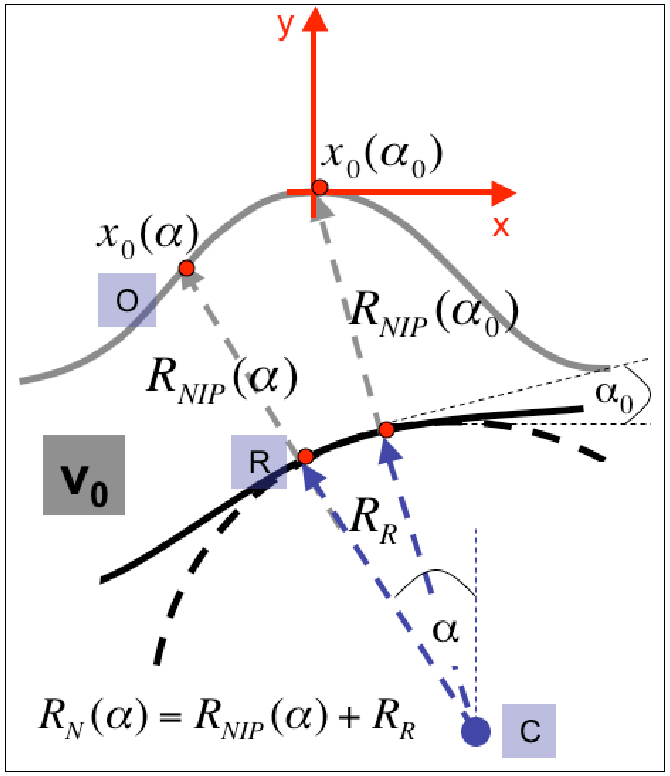

Figure 11: NIP-ray leaving the reflector of equation $y_R = g(x_R)$.

Useful trigonometric relations

With the help of figure (12), we see that

$$\tan\alpha = \frac{x_C - x_R}{g(x_R) - y_C}, \tag{28}$$

where

$$x_R = x_0 + R_{NIP}(\alpha)\sin\alpha, \quad y_R = -\left[Kx_0^2 + R_{NIP}(\alpha)\cos\alpha\right], \tag{29}$$

and

$$x_C = R_N \sin\alpha_0, \quad y_C = -R_N \cos\alpha_0. \tag{30}$$

Remark that with this notation $x_0 = x_0(\alpha)$ and $x_R = x_R(\alpha)$.

In addition, the radius of curvature of the reflector being *constant* around R, we can write $R_R = R_N - R_{NIP} = R_N(\alpha) - R_{NIP}(\alpha)$, so that, for deep angles near α_0, we have

$$\frac{x_R}{\sin\alpha} = R_N\left(\frac{\sin\alpha_0}{\sin\alpha} - 1\right) + R_{NIP}. \tag{31}$$

Computing $x_0(\alpha)$ for a NIP-ray reaching the curved surface

We want to determine $x_0 = x_0(\alpha)$, the impact point at the surface of a NIP-ray traveling near the reference one, figure (12):

$$\begin{bmatrix} x_0 \\ -Kx_0^2 \end{bmatrix} = \begin{bmatrix} x_R \\ g(x_R) \end{bmatrix} + \lambda \begin{bmatrix} -\tan\alpha \\ 1 \end{bmatrix}. \tag{32}$$

Eliminating λ in (32), with the help of equations (28), (29) and (30), we finally find:

$$x_0(\alpha) = \frac{1}{2K\tan\alpha}\left\{1 - \sqrt{1 + 4KR_N\tan\alpha\,(\tan\alpha\cos\alpha_0 - \sin\alpha_0)}\right\}. \tag{33}$$

Observe that, first, $x_0(\alpha_0) = 0$ and, second, taking the limit $K \to 0$ we recover the planar case, equation (6).

Computing $R_{NIP}(\alpha)$ for a NIP-ray reaching the curved surface

We start with equation (32) and observe that $\overline{OR} = |\lambda|/\cos\alpha$ and $\lambda = -[Kx_0^2 + g(x_R)]$. Thus we can write:

$$R_{NIP}(\alpha) = \frac{Kx_0^2 + g(x_R)}{\cos\alpha}. \tag{34}$$

Using (31) and (33), equation (34) takes the form

$$\begin{aligned} R_{NIP}(\alpha) \quad = \quad & R_{NIP} + R_N \left(\frac{\sin\alpha_0}{\sin\alpha} - 1 \right) - \\ & \frac{\cos\alpha}{2K\sin^2\alpha} \left\{ 1 - \sqrt{1 + 4KR_N \tan\alpha\,(\tan\alpha\cos\alpha_0 - \sin\alpha_0)} \right\}. \end{aligned} \tag{35}$$

Observe that, first, $R_{NIP}(\alpha_0) = R_{NIP}$ and, second, taking the limit $K \to 0$ we recover the planar case, equation (5).

First acquisition configuration: $h = 0$

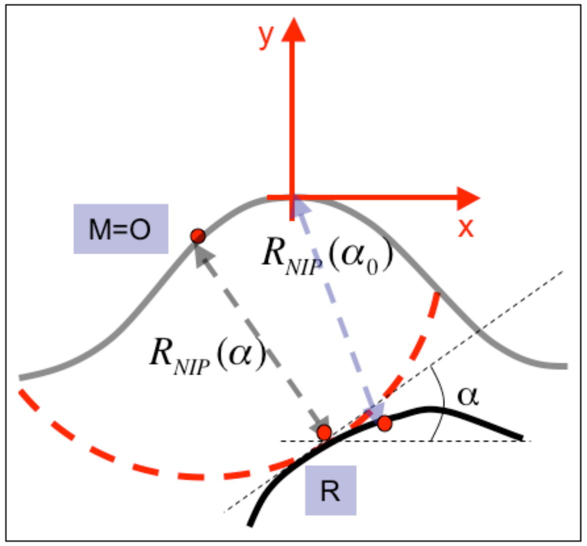

Figure 12: Zero-offset acquisition on a curved surface.

The line of equal reflection time, tangent to the reflector, is the circle centered in x_m with radius R_{NIP}. In this source-receiver configuration, we have for any deep α

$$x_m(\alpha) = x_0(\alpha), \qquad \frac{v_0 t}{2} = R_{NIP}(\alpha). \tag{36}$$

To set up the paraxial approximation, let us perturb $x_0(\alpha)$, equation (33), and $R_{NIP}(\alpha)$, equation (35), around the reference angle α_0 corresponding to $x_m(\alpha_0) = x_0 = 0$.

Paraxial approximation for $h = 0$ (first part)

The second-order Taylor series expansion of equations (36) take the form

$$\begin{aligned} t(\alpha) &= \frac{2R_{NIP}}{v_0} + \frac{2R_N}{v_0} \tan\alpha_0 \, (\alpha - \alpha_0) + \\ & \frac{R_N}{v_0} \left(1 + 2\tan^2\alpha_0 - \frac{2KR_N}{\cos^3\alpha_0}\right) (\alpha - \alpha_0)^2 + O(3), \end{aligned} \tag{37}$$

$$\begin{aligned} x_m(\alpha) &= \frac{R_N}{\cos\alpha_0} \, (\alpha - \alpha_0) + \\ & \frac{R_N \sin\alpha_0}{\cos^2\alpha_0} \left(1 - \frac{KR_N}{\cos\alpha_0}\right) (\alpha - \alpha_0)^2 + O(3), \end{aligned} \tag{38}$$

generalizing equations (8) and (9) for the case of a surface with a local curvature $\kappa = 2K$ at $x_0 = 0$.

Paraxial approximation for $h = 0$ (second part)

Using Lagrange formula (10), the inversion of (38) provides the following relation between α and x_m, valid in the neighborhood of the reference NIP-ray:

$$\alpha - \alpha_0 = \frac{\cos\alpha_0}{R_N} x_m + \frac{\sin\alpha_0}{R_N^2}(KR_N - \cos\alpha_0)x_m^2 + O(3). \tag{39}$$

After the substitution of (39) into (37), the *zero-offset* time of flight for *homogeneous* media can now be represented as a function of the midpoint coordinate x_m:

$$t(x_m) = 2\,\frac{R_{NIP}}{v_0} + 2\,\frac{\sin\alpha_0}{v_0} x_m + \frac{\cos\alpha_0}{v_0 R_N}\left(\cos\alpha_0 - 4KR_N\right) x_m^2 + O(3), \tag{40}$$

$$\begin{aligned} t^2(x_m) &= 4\,\frac{R_{NIP}^2}{v_0^2} + 8\,\frac{R_{NIP}\sin\alpha_0}{v_0^2} x_m + \\ &\quad \frac{4}{v_0^2}\left(\frac{R_{NIP}\cos^2\alpha_0 + R_N\sin^2\alpha_0}{R_N} - 2KR_{NIP}\cos\alpha_0\right) x_m^2 + O(3). \end{aligned} \tag{41}$$

Equations (40) and (41) are respectively the *parabolic* and the *hyperbolic* zero-offset expansions for the case with a local curvature $\kappa = 2K$ at $x_0 = 0$.

Second acquisition configuration: $x_m = 0$ and $y_m = -Kh^2$ (first part)

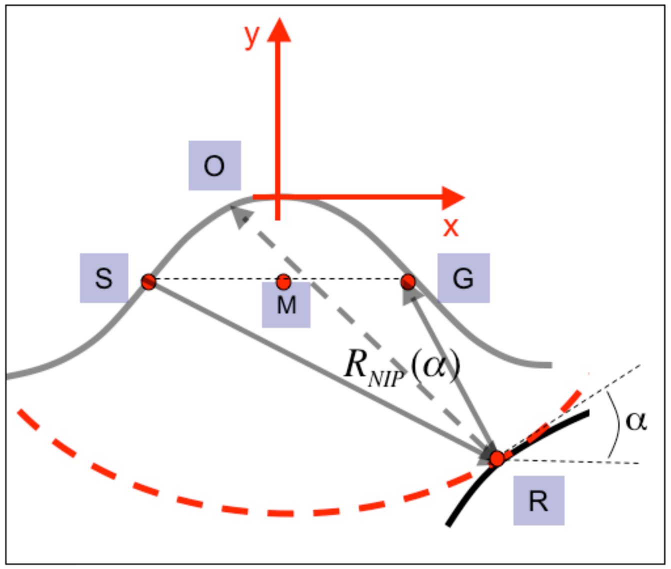

Figure 13: Acquisition with offset h on a curved surface.

The line of equal reflection time, tangent to the reflector at point R, is the ellipse centered at the midpoint M with foci on source and receiver positions:

$$\frac{x_R^2}{v_0^2\ t^2} + \frac{\left(y_R + Kh^2\right)^2}{v_0^2\ t^2 - 4h^2} = \frac{1}{4}, \quad \text{where} \quad \frac{x_R}{y_R + Kh^2} = -\frac{v_0^2\ t^2}{v_0^2\ t^2 - 4h^2} \tan\alpha, \qquad (42)$$

The coordinates (x_R, y_R) of the reflecting point R are given by (29).

Second acquisition configuration: $x_m = 0$ and $y_m = -Kh^2$ (second part)

Using (29), the system of equations (42) provides the following solution:

$$\left(\frac{v_0 t}{2}\right)^2 = h^2 + \frac{\Delta y_R^2}{\cos^2\alpha} - \Delta y_R \tan\alpha \left[x_0(\alpha) - K(x_0^2 - h^2)\right], \tag{43}$$

$$x_0(\alpha) = K\left[x_0^2(\alpha) - h^2\right]\tan\alpha - \Gamma(\alpha)\left[\sqrt{\frac{h^2}{\Gamma^2(\alpha)} + 1} - 1\right], \tag{44}$$

where

$$\Delta y_R = K\left[x_0^2(\alpha) - h^2\right] - R_{NIP}\cos\alpha, \qquad \Gamma(\alpha) = \frac{\Delta y_R}{2\sin\alpha\cos\alpha}.$$

With the help of expression (33), eliminating x_0 in both equations (43) and (44), we are ready to construct the paraxial approximation of $t = t(\alpha)$ and $h = h(\alpha)$, developing in Taylor series these two functions around α_0.

Paraxial approximation for $x_m = 0$ (first part)

The Taylor series expansion in α of equation (43) takes the form

$$\left(\frac{v_0 t}{2}\right)^2 = R_{NIP}^2 + K^2 h^2 + \tan\alpha_0\ R_{NIP} R_N\ (\alpha-\alpha_0) + \left\{1 - \frac{K R_{NIP}}{\cos\alpha_0}(1+\cos^2\alpha_0) - K\frac{\sin\alpha_0}{\cos^2\alpha_0}\left[R_{NIP} + \cos^2\alpha_0\ (R_N - R_{NIP})\right](\alpha-\alpha_0)\right\} h^2 + O(2). \tag{45}$$

Observe that (44) may be recast as a second-order polynomial in h^2, whose admissible root is approximated as follows

$$h^2 = \frac{R_{NIP} R_N}{\sin\alpha_0\ (R_{NIP} K - \cos\alpha_0)}(\alpha-\alpha_0) + O(2),$$

so that, after inversion,

$$\alpha - \alpha_0 = \frac{\sin\alpha_0\ (R_{NIP} K - \cos\alpha_0)}{R_{NIP} R_N} h^2 + O(4). \tag{46}$$

Paraxial approximation for $x_m = 0$ (second part)

Finally, after substitution of (46) into (45), we obtain the *hyperbolic* expression of the *time of flight*, as a function of the offset h, for a trajectory in a *homogeneous* medium near the reference NIP-ray:

$$t^2(h) = \left(\frac{2R_{NIP}}{v_0}\right)^2 + \frac{4\cos\alpha_0}{v_0^2}\left(\cos\alpha_0 - 2KR_{NIP}\right)h^2 + O(4). \tag{47}$$

From the power-series expansion of the square root of expression (47), we derive the *parabolic* form of the *time of flight*:

$$t(h) = \frac{2R_{NIP}}{v_0} + \frac{\cos\alpha_0}{v_0\; R_{NIP}}\left(\cos\alpha_0 - 2KR_{NIP}\right)h^2 + O(4). \tag{48}$$

Equations (47) and (48) generalize equations (17) and (18) for an acquisition on a surface with curvature $\kappa = 2K$ at $x_0 = 0$, figure (13).

Curved surface, time of flight in homogeneous media: paraxial approximation

From the Taylor-series expansion (7), collecting (40) and (48), we obtain the *parabolic* approximation, valid near the reference NIP-ray in a constant-velocity media:

$$\begin{aligned} t(x_m, h) \quad = \quad & \frac{2R_{NIP}}{v_0} + \frac{\cos\alpha_0}{v_0\ R_{NIP}}\left(\cos\alpha_0 - 2KR_{NIP}\right)h^2 + \\ & \frac{2\sin\alpha_0}{v_0}x_m + \frac{\cos\alpha_0}{v_0 R_N}\left(\cos\alpha_0 - 4KR_N\right)x_m^2 + O(3). \end{aligned} \tag{49}$$

Similarly, using (41) and (47), we derive the *hyperbolic* approximation:

$$\begin{aligned} t^2(x_m, h) \quad = \quad & \frac{4\ R_{NIP}^2}{v_0^2} + \frac{4\cos\alpha_0}{v_0^2}\left(\cos\alpha_0 - 2KR_{NIP}\right)h^2 + 8\ \frac{R_{NIP}\sin\alpha_0}{v_0^2}x_m + \\ & \frac{4}{v_0^2}\left(\frac{R_{NIP}\cos^2\alpha_0 + R_N\sin^2\alpha_0}{R_N} - 2KR_{NIP}\cos\alpha_0\right)x_m^2 + O(3). \end{aligned} \tag{50}$$

Remark that setting $K = 0$, we recover the expressions obtained for a flat acquisition surface provided by equations (19) and (20).

Curved surface, time of flight in non-homogeneous media: paraxial approximation

The *correction* of the time of flight $t(x_m, h)$ in a real medium requires the use of an *auxiliary* homogeneous model, leading again to the time delay (23). Therefore, from (49) and (50) we obtain the modified parabolic and hyperbolic expressions, valid for in-homogeneous media, which take into account the ground surface curvature:

$$\begin{aligned} t(x_m, h) &= t_0 + \frac{\cos\alpha_0}{v_0\ R_{NIP}}\left(\cos\alpha_0 - 2KR_{NIP}\right)h^2 + \\ & \frac{2\sin\alpha_0}{v_0}x_m + \frac{\cos\alpha_0}{v_0 R_N}\left(\cos\alpha_0 - 4KR_N\right)x_m^2 + O(3), \end{aligned} \tag{51}$$

and

$$\begin{aligned} \left[t(x_m, h) - \left(t_0 - \frac{2R_{NIP}}{v_0}\right)\right]^2 &= \\ \frac{4\ R_{NIP}^2}{v_0^2} + \frac{4\cos\alpha_0}{v_0^2}\left(\cos\alpha_0 - 2KR_{NIP}\right)h^2 + & \\ \frac{8R_{NIP}\sin\alpha_0}{v_0^2}x_m + \frac{4}{v_0^2}\left(\frac{R_{NIP}\cos^2\alpha_0 + R_N\sin^2\alpha_0}{R_N} - 2KR_{NIP}\cos\alpha_0\right)x_m^2 + O(3). & \end{aligned} \tag{52}$$

General conclusion

The seismic reflection-time derivation presented in this document provides an analytic solution *independent* of the subsurface macro-velocity model. The resulting expressions are defined, for an arbitrary source-receiver pair, in the midpoint-offset domain.

To reach this goal, firstly, we started with the homogeneous problem where this derivation was based on a paraxial approximation of $t(x_m, h)$, the reflection time, assuming down-going and up-going ray trajectories near a *reference* NIP-ray. This last trajectory was characterized by three parameters denoted as α_0, R_{NIP} and R_N.

Secondly, a homogeneous subsurface *reference model* was designed to behave as the real medium under examination, in the sense that NIP- and N-waves, and their images in the reference world reach the surface with different time of flight but with the same radii of curvature, R_{NIP} and R_N, and emergence angle α_0. In addition, these waves are assumed to propagate with the same velocity near the surface.

Consequently, close to the surface, traveled distances are the same in both models, a feature which provides the estimate of the *time correction* $\Delta t(x_m, h)$ between the true non-homogeneous medium and the reference one, leading to the proper expression of time of flight $t(x_m, h)$ as a function of the three parameters α_0, R_{NIP} and R_N.

References

- G. Höcht, J. Mann and R. Jäger, *The Common Reflection Surface Stack - Part I: Theory*, Wave Inversion Technology (WIT), Report N. 2, pp. 7-14, 1999.
- G. Höcht, E. de Bazelaire, P. Majer and P. Hubral, *Seismic and Optics: Hyperbolae and Curvatures*, J. of Applied Geophysics, **42**, pp. 261-281, 1999.
- P. Chira, M. Tygel, Y. Zhang and P. Hubral, *Analytic CRS Formula for a 2D Curved Measurement Surface and Finite-offset Reflections*, J. of Seismic Exploration, **10**, pp. 245-262., 2001.
- V. Grosfeld, R. Biloti, L. T. Santos and M. Tygel, *Topographic Effect Correction Using CRS Parameters*, 7th International Congress of the Brazilian Geophysical Society, Salvador, Brazil, 2001.
- *Maple 6 Programming Guide*, Waterloo Maple Inc., 2000.